Journal of Solid State Chemistry **148,** 129–134 (1999)
Article ID jssc.1999.8397, available online at http://www.idealibrary.com on IDEAL®

Structural Phase Transition in Adipic Acid

R. Srinivasa Gopalan, P. Kumaradhas, and G. U. Kulkarni[1]

Chemistry and Physics of Materials Unit, Jawaharlal Nehru Centre for Advanced Scientific Research, Jakkur, Bangalore 560 064, India

Received February 5, 1999; in revised form May 11, 1999; accepted May 24, 1999

The structure of adipic acid undergoing phase transition at ~136 K has been investigated using single-crystal x-ray diffraction. On lowering the temperature, the *a* parameter of the room temperature monoclinic cell decreases by ~0.25 Å. Accompanying the transition, the *b* parameter nearly triples while *a* reverts back to the room temperature value. Two-thirds of the molecules in the structure loses center of symmetry. Packing diagrams of the high- and low-temperature phases on superposition reveal that there exist alternating domains perpendicular to the *b* direction, which contain molecules with and without symmetry. Unsymmetric molecules show displacements along the *ac* diagonal. Intermolecular hydrogen contacts involving carboxylic oxygens and the methylene hydrogens seem to increase interchain interactions in the low-temperature phase.

INTRODUCTION

Structural investigation of crystalline solids undergoing phase transformation has been one of the classical areas of research among both chemists and physicists (1). Many inorganic as well as organic crystals exhibiting order–disorder or displacive transitions have been investigated in the past (2). Molecular solids in particular are more interesting in that they often crystallize in different structural forms and exhibit polymorphic transformations (3, 4). It is indeed exciting to examine in such crystals how molecules move in a concerted fashion following lattice transformation, accommodating minimum possible distortion in their own geometry. For example, single-crystal to single-crystal transformations have been investigated in *p*-terphenyl (5), biphenyl (6), and *s*-triazine (7). This, however, is not always the case.

Alkanedioic acids are good examples of molecular solids that exhibit polymorphism (8, 9). The first few members of this series except adipic acid are known to exist in two forms, α and β, the latter being more stable at room temperature. In the β form other than that of malonic, the molecule possesses an internal symmetry. In the even-membered case, there is an inversion center on the central C–C bond and the molecular backbone is virtually planar. The odd members on the other hand, have a twofold axis of symmetry through the central carbon atom and the chain is slightly twisted. Malonic acid however, does not posses any element of symmetry and the two carboxylic groups are almost perpendicular to each other. The $\beta \rightarrow \alpha$ transitions for the dicarboxylic acids occur in the 340 to 410 K temperature range. In the case of odd acids, the twofold axis of symmetry is lost in the high-temperature phase while the even acids retain their inversion center. Besides polymorphism, the dicarboxylic acids have been found to exhibit many interesting properties such as alternation in the melting point.

Adipic acid has not been studied in detail. Morrison and Robertson (10) first reported the structure of the room-temperature phase, which was further refined by Housty and Hospital (11). Recently, Ohki *et al.* (12) reported that adipic acid undergoes a phase transformation at about 136 K. The thermal anomaly associated with the transition was found to be small and exhibited a λ-type behavior without hysterisis, indicating the phase transition to be of second or higher order. Raman spectroscopy on powder samples showed the appearance of a weak band below the transition whose intensity increased on further cooling. The authors also reported that single-crystal studies were fruitless as the crystals cracked on cooling near the phase transition temperature.

We independently chanced upon the phase transition in adipic acid while collecting low-temperature data for an electron density study on various dicarboxylic acids. We have investigated the structural aspects of the phase transition and have therefore carried out x-ray diffraction measurements on both the high- and the low-temperature phases using the same crystal. Our results have shown that the phase transition is induced due to increased interchain interactions involving carboxylic oxygens and methylene hydrogens.

EXPERIMENTAL

Adipic acid crystals were grown by slow evaporation of a saturated ethyl acetate solution (10). The crystals were

[1] To whom correspondence should be addressed. E-mail: kulkarni@jncasr. ac.in.

0022-4596/99 $30.00

colorless and cuboidal in shape. X-ray diffraction intensities were measured by ω scans using a Siemens three-circle diffractometer attached with a CCD area detector and a graphite monochromator for the Mo$K\alpha$ radiation (50 kV, 40 mA). The crystal was cooled on the diffractometer using a stream of cold nitrogen gas from a vertical nozzle. During the measurement, the temperature of the crystal was held constant at a desired value within ± 0.5 K. The phase transition at 136 K often induced cracking and shattering of the crystals. In order to achieve a single-crystal to single-crystal transition, we made a number of attempts by slow cooling of the crystals (~ 3 K/h) especially near the transition temperature. The crystal chosen could be taken through several cycles of cooling and heating.

Initially at a given temperature, the unit-cell parameters and the orientation matrix of the crystal were determined using ~ 40 strong reflections from 25 frames collected over a small ω scan of 7.5° sliced at 0.3° intervals. A hemisphere of reciprocal space was then collected using the SMART software (13) with the 2θ setting of the detector at 28°. The data reduction was performed using the SAINT program (13) and the orientation matrix along with the detector and the cell parameters were refined for every 40 frames on all the measured reflections. The crystal structures were solved by the direct methods using the SHELXTL program (14). The structures were refined by full-matrix least squares on F^2. All the nonhydrogens were refined anisotropically. The hydrogen atoms were located by difference Fourier method and were refined isotropically. The crystal data and the experimental details are listed in Table 1. Bond lengths, bond angles, and torsion angles for the high- and low-temperature phases are listed Table 2. Hydrogen bond contacts are listed in Table 3.

TABLE 1
Crystal Data and Experimental Details

Chemical formula		$C_6H_{10}O_4$	
Formula weight		146.064	
		145 K	116 K
Cell setting		Monoclinic	Monoclinic
Space group		$P2_1/n$	$P2_1/n$
a (Å)		7.1761(11)	7.4282(2)
b (Å)		5.1501(8)	14.9925(1)
c (Å)		10.0158(16)	10.1000(3)
β (°)		111.13(2)	111.45(1)
Volume (Å^3)		345.27(1)	1046.90(5)
ρ (g cm^{-3})		1.406	1.391
z		4	4
Radiation type		Mo$K\alpha$	
Wave length (Å)		0.71073	
μ (mm^{-1})		0.12	0.12
Crystal form		Cuboidal	Cuboidal
Crystal size (mm)		$0.4 \times 0.3 \times 0.2$	$0.4 \times 0.3 \times 0.2$
Crystal color		Colorless	Colorless
Data collection			
Diffractometer		Siemens CCD	
Data collection		ω scan	
Crystal–detector distance (cm)		5.0	
No. of measured reflections		1891	5678
No. of independent reflections		752	2236
No. of observed reflections		670	2234
R_{merge}		0.039	0.046
R_{int}		0.045	0.05
θ_{max} (°)		28.0	27.6
Range of h, k, l		$-9 \rightarrow h \rightarrow 9$	$-8 \rightarrow h \rightarrow 9$
		$-5 \rightarrow k \rightarrow 6$	$-16 \rightarrow k \rightarrow 19$
		$-13 \rightarrow l \rightarrow 12$	$-13 \rightarrow l \rightarrow 12$
Refinement			
Refinement on F^2			
	$R(F)$	0.046	0.061
	w$R(F^2)$	0.135	0.169
	S	1.12	1.09
Weights used	w	0.08, 0.10	0.07, 1.09
No. of reflections used in the refinement		668	1591
No. of parameters refined		67	197
$(\Delta/\sigma)_{max}$		0.06	0.07
$\Delta\rho_{max}$ (eÅ^{-3})		0.32	0.37
$\Delta\rho_{min}$(eÅ^{-3})		−0.26	−0.32

RESULTS AND DISCUSSION

Adipic acid crystallizes in a centrosymmetric monoclinic space group ($P2_1/n$) with two molecules per unit cell ($a = 7.3672(3)$, $b = 5.1492(2)$, $c = 10.0090(2)$ Å and $\beta = 110.569(1)$°). In Fig. 1, we show variations in the cell parameters and the crystal density with temperature. As the temperature is decreased from the ambient to close to the transition temperature, the a parameter decreases by ~ 0.25 Å while b and c show only small variations (Fig. 1a). Below the transition at 136 K, the cell is still monoclinic with the same space group. As we notice in Table 1, the a parameter reverts back to its room-temperature value while the c parameter remains essentially unchanged. Interestingly, the b parameter nearly triples to 14.9925(1) Å accompanying the transition. It is shorter by ~ 0.5 Å from the ideal tripled value. The angle β shows a gradual increase on cooling and exhibits a cusp near the transition while the density ρ increases steadily (Fig. 1b). The phase transition therefore appears to be of second order, which also explains the necessity of slow cooling of the crystal.

In Fig. 2, we show the asymmetric units used in structure refinement of the high- and the low-temperature phases. We see from Fig. 2 that the asymmetric unit in the high-temperature phase contains only half the adipic molecule (10) and the other half is generated by inversion. We see from Table 2 that the C–C bond length increases gradually from 1.498(2) for the carboxylic linkage to 1.520(3) for the central bond. The carbon backbone is nonplanar. The torsion angle C(1)–C(2)–C(3)–C(3′) is $\sim 173.2(1)$° while the inner torsion angle C(2)–C(3)–C(3′)–C(2′) is 180°. The plane containing

TABLE 2
Bond Lengths, Bond Angles, and Torsion Angles of the High- and Low-Temperature Phases of Adipic Acid

Bond lengths (Å)	145 K	116 K
O1–C1	1.224(2)	1.234(3)
O2–C1	1.315(2)	1.324(4)
O2–H2	0.98(3)	0.94(4)
C1–C2	1.498(2)	1.515(4)
C2–C3	1.515(2)	1.524(4)
C2–H2A	0.97(2)	1.00(3)
C2–H2B	0.98(2)	0.99(3)
C3–H3A	0.96(2)	0.99(3)
C3–H3B	1.00(2)	0.98(3)
O3–C4		1.232(3)
O4–C4		1.325(4)
O4–H4		0.94(4)
O5–C9		1.232(3)
O6–C9		1.327(4)
O6–H6		0.93(5)
C4–C5		1.512(4)
C5–C6		1.527(4)
C5–H5A		1.00(3)
C5–H5B		1.02(3)
C6–C7		1.542(4)
C6–H6A		1.02(3)
C6–H6B		0.99(4)
C7–C8		1.527(4)
C7–H7A		0.99(3)
C7–H7B		1.03(3)
C8–C9		1.510(4)
C8–H8A		0.99(3)
C8–H8B		0.96(3)

Bond angles (°)	145 K	116 K
C1–O2–H2	108(2)	107(2)
O1–C1–O2	123.0(1)	123.2(2)
O2–C1–C2	113.2(1)	113.1(2)
O1–C1–C2	123.8(1)	123.7(3)
C1–C2–H2B	105(1)	107(2)
C1–C2–H2A	107(1)	107(2)
C1–C2–C3	114.1(1)	114.3(2)
H2A–C2–H2B	109(2)	108(2)
C3–C2–H2B	110(1)	111(2)
C3–C2–H2A	112(1)	110(2)
C2–C3–H3B	110(1)	110(2)
C2–C3–H3A	111(1)	110(2)
H3A–C3–H3B	107(1)	107(3)
C4–O4–H4		111(2)
C9–O6–H6		108(3)
O3–C4–O4		123.5(3)
O4–C4–C5		112.8(2)
O3–C4–C5		123.7(3)
C4–C5–H5B		107(2)
C4–C5–H5A		104(2)
C4–C5–C6		114.2(2)
H5A–C5–H5B		105(2)
C6–C5–H5B		111(2)
C6–C5–H5A		115(2)

TABLE 2—*Continued*

Bond angles (°)	145 K	116 K
C5–C6–H6B		110(2)
C5–C6–H6A		109(2)
C5–C6–C7		111.8(2)
H6A–C6–H6B		108(3)
C7–C6–H6B		109(2)
C7–C6–H6A		108(2)
C6–C7–H7B		110(2)
C6–C7–H7A		110(2)
C6–C7–C8		111.0(2)
H7A–C7–H7B		105(2)
C8–C7–H7B		110(2)
C8–C7–H7A		111(2)
C7–C8–H8B		110(2)
C7–C8–H8A		110(2)
C7–C8–C9		114.1(2)
H8A–C8–H8B		110(3)
C9–C8–H8B		106(2)
C9–C8–H8A		108(2)
O6–C9–C8		112.8(2)
O5–C9–C8		124.0(3)
O5–C9–O6		123.2(2)

Torsion angles (°)	145 K	116 K
H2–O2–C1–O1	4(2)	−6(3)
H2–O2–C1–C2	−176(2)	175(3)
O2–C1–C2–C3	173.5(1)	177.1(3)
O1–C1–C2–C3	−6.9(2)	−2.0(4)
O2–C1–C2–H2A	49(1)	−61(2)
O1–C1–C2–H2A	−131(1)	120(2)
O2–C1–C2–H2B	−66(1)	55(2)
O1–C1–C2–H2B	114(1)	−125(2)
C1–C2–C3–H3A	66(1)	−60(2)
C1–C2–C3–H3B	−52(1)	57(2)
H2A–C2–C3–H3B	70(2)	−63(3)
H2A–C2–C3–H3A	−173(2)	179(3)
H2B–C2–C3–H3B	−170(2)	178(3)
H2B–C2–C3–H3A	−52(2)	60(3)
H4–O4–C4–O3		2(3)
H4–O4–C4–C5		−178(3)
H6–O6–C9–O5		−3(3)
H6–O6–C9–C8		178(3)
O4–C4–C5–C6		170.0(2)
O3–C4–C5–C6		−10.2(4)
O4–C4–C5–H5A		43(2)
O3–C4–C5–H5A		−137(2)
O4–C4–C5–H5B		−68(2)
O3–C4–C5–H5B		112(2)
C4–C5–C6–C7		−172.3(2)
C4–C5–C6–H6A		68(2)
C4–C5–C6–H6B		−50(2)
H5A–C5–C6–H6B		70(3)
H5A–C5–C6–H6A		−172(3)
H5A–C5–C6–C7		−52(2)
H5B–C5–C6–H6B		−171(3)
H5B–C5–C6–H6A		−53(3)
H5B–C5–C6–C7		68(2)

TABLE 2—*Continued*

Torsion angles (°)	145 K	116 K
C5–C6–C7–C8		−175.7(2)
C5–C6–C7–H7A		61(2)
C5–C6–C7–H7B		−54(2)
H6A–C6–C7–H7B		66(3)
H6A–C6–C7–H7A		−179(3)
H6A–C6–C7–C8		−55(2)
H6B–C6–C7–H7B		−177(3)
H6B–C6–C7–H7A		−62(3)
H6B–C6–C7–C8		62(2)
C6–C7–C8–C9		173.9(2)
C6–C7–C8–H8A		−65(2)
C6–C7–C8–H8B		56(2)
H7A–C7–C8–H8B		178(3)
H7A–C7–C8–H8A		58(3)
H7A–C7–C8–C9		−63(2)
H7B–C7–C8–H8B		−66(3)
H7B–C7–C8–H8A		173(3)
H7B–C7–C8–C9		53(2)
C7–C8–C9–O6		−172.2(2)
C7–C8–C9–O5		8.2(4)
H8A–C8–C9–O6		66(2)
H8A–C8–C9–O5		−114(2)
H8B–C8–C9–O6		−51(2)
H8B–C8–C9–O5		129(2)

the carboxylic group makes an angle of ∼7° with the C(1)–C(2)–C(3) plane. In the low-temperature phase on the other hand, we found that the asymmetric unit is composed of one and a half molecule. The half-molecule fragment resembles the asymmetric unit of the high-temperature phase with the center of inversion lying on it. It is however, relatively more planar with the torsion angle C(1)–C(2)–C(3)–C(3′) being 177.0(1)°. The angle made by the carboxylic group is also smaller, ∼3°. The full-molecule fragment of the low-temperature asymmetric unit obviously does not contain a center of inversion. The molecular backbone is buckled, the torsion angles being 172.3(2)°, 175.7(2)°, and 173.9(2)° along its length. The carboxylic groups also deviate significantly from the mean plane of the hydrocarbon chain (∼10°). We notice that the central C–C bond of this molecule is close to the ideal tetrahedral value of 1.54 Å (Table 2). The bond angles do not change appreciably following the phase transition.

We made use of the simple relationship between the high- and low-temperature cells and superimposed the crystal structures in order to visualize the deformation of one structure into the other involving translations and rotations of the individual molecules. In Fig. 3, we show such a packing diagram along with the unit cells. We observe that in the low-temperature phase, the half-molecule fragment of the asymmetric unit generates molecules which roughly remain in place during phase transition while those generated by the full-molecule fragment show noticeable displacements perpendicular to the screw axis and along the *ac*-diagonal (by ∼0.8 Å) leading to tripling of the unit cell in the *b* direction. Therefore, the deformation occurs in the alternating domains labeled "FM" in Fig. 3. The HM domains closely resemble the high-temperature structure. The domain interface typifies new interchain interactions resulting from the phase transition. In the regions enclosed by circles in Fig. 3

TABLE 3
Hydrogen Bond Contacts in the High- and Low-Temperature Phases

D–H···*A*	H···*A* (Å)	∠D–H···*A* (°)	D–H···*A*	H···*A* (Å)	∠D–H···*A* (°)
145 K			116 K		
O(2)–H(2)···O(1)^{b}	1.72(3)	173(3)	O(2)–H(2)···O(1)^{e}	1.71(4)	168(3)
			O(6)–H(6)···O(3)^{h}	1.68(5)	170(4)
			O(4)–H(4)···O(5)^{j}	1.70(4)	176(3)
C(3)–H(3A)···O(1)^{c}	2.92(3)	120(3)	C(5)–H(5A)···O(1)^{a}	2.86(3)	147(2)
			C(5)–H(5B)···O(1)^{b}	2.85(3)	131(2)
			C(8)–H(8A)···O(1)^{f}	2.97(3)	141(2)
			C(7)–H(7A)···O(3)^{i}	2.87(3)	120(2)
			C(2)–H(2A)···O(5)^{k}	2.88(3)	145(2)
C(2)–H(2A)···O(2)^{d}	2.73(3)	108(3)	C(8)–H(8B)···O(2)^{g}	2.71(3)	115(2)
C(3)–H(3B)···O(2)^{d}	2.82(3)	120(3)	C(7)–H(7B)···O(2)^{g}	2.65(3)	121(2)
			C(2)–H(2A)···O(4)^{e}	2.74(3)	116(2)
			C(5)–H(5A)···O(6)^{l}	2.81(3)	103(2)
			C(6)–H(6B)···O(6)^{l}	2.85(3)	119(2)

Note. Symmetry: (*a*) x, y, z; (*b*) $-x, -y, 1-z$; (*c*) $1/2-x, -1/2-y, 1/2-z$; (*d*) $-1/2-x, 1/2+y, 1/2-z$; (*e*) $1-x, -y, 1-z$; (*f*) $1/2-x, 1/2+y, 3/2-z$; (*g*) $x-1, y, z$; (*h*) $x, y, 1+z$; (*i*) $1/2-x, 1/2-y, 1/2+z$; (*j*) $x, y, z-1$; (*k*) $1+x, y, z$; (*l*) $1/2+x, 1/2-y, -1/2-z$.

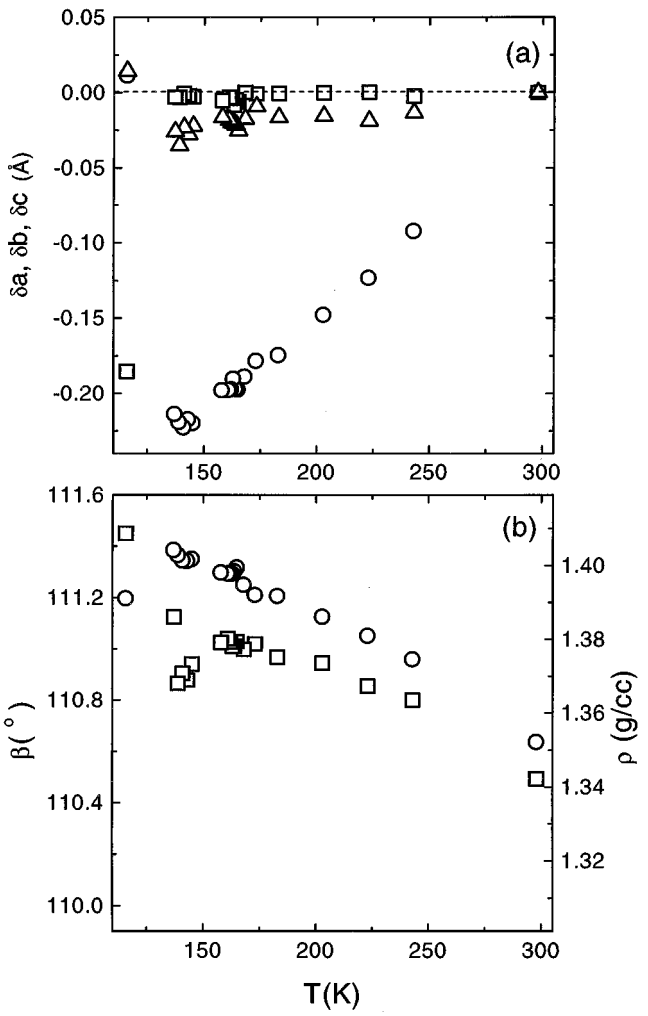

FIG. 1. Variations with respect to the room temperature values in (a) *a*, circles; *b*, squares; *c*, triangles and (b) *β*, squares; *ρ*, circles with temperature. The datapoint (square) at 116 K in (a) refers to one-third of the tripled *b* parameter in the low-temperature phase.

for instance, methylene hydrogens from the FM domain appear to have moved between the carboxylic groups in the HM domain.

The intermolecular hydrogen contacts of the dimeric units involving the carboxylic groups run perpendicular to the *b* axis and are affected to some extent by the phase transition (see Table 3). In the high-temperature phase, the intermolecular H(2)···O(1) distance is 1.72(3) Å with ∠O(2)–H(2)···O(1) of 173(3)°. Below transition, the carboxylic group in the HM domain exhibits a H···O contact of 1.71 Å with an angle of 168(3)° while that in the FM domain has contacts at 1.68(5) and 1.70(4) Å with angles of 170(4)° and 176(3)°, respectively. In addition to the O–H···O contacts, we observe up to six C–H···O contacts per-molecule in the range 2.7 and 2.9 Å in both the high- and the low-temperature phases (Table 3). The difference is that in the low-temperature phase, the contact angles are considerably higher making C–H···O interactions more favorable.

From the above discussion, it appears that at room temperature there are only moderate side-chain interactions compromising with the allowable strain in the molecule. On cooling the crystal, the side-chain interactions increase because of closer proximity down to a temperature where the crystal undergoes phase transition giving rise to two types of molecules. It is as though the molecules with evenly distributed strain in the high-temperature phase segregate into two domains comprising unstrained molecules in one domain (HM) and highly strained molecules without inversion symmetry in the other (FM). The resulting molecular displacements seem to favor stronger interchain interactions. Preliminary results from a charge density analysis on the high- and low-temperature phases show bonding interactions between the methylene and the carboxylic oxygens in the low-temperature phase. A detailed work is in progress.

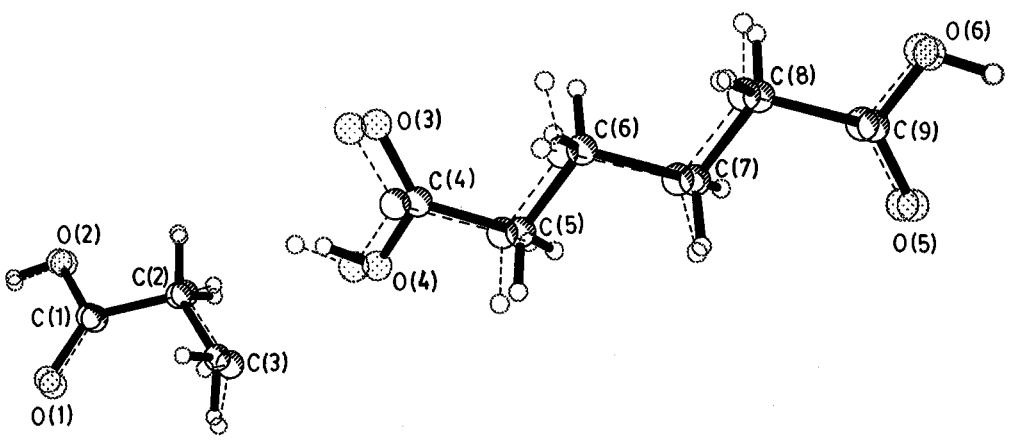

FIG. 2. Asymmetric units of adipic acid in the high- (dashed) and the low-temperature (solid line) phases. A 2_1 related full molecule of the high-temperature phase is also shown for comparison.

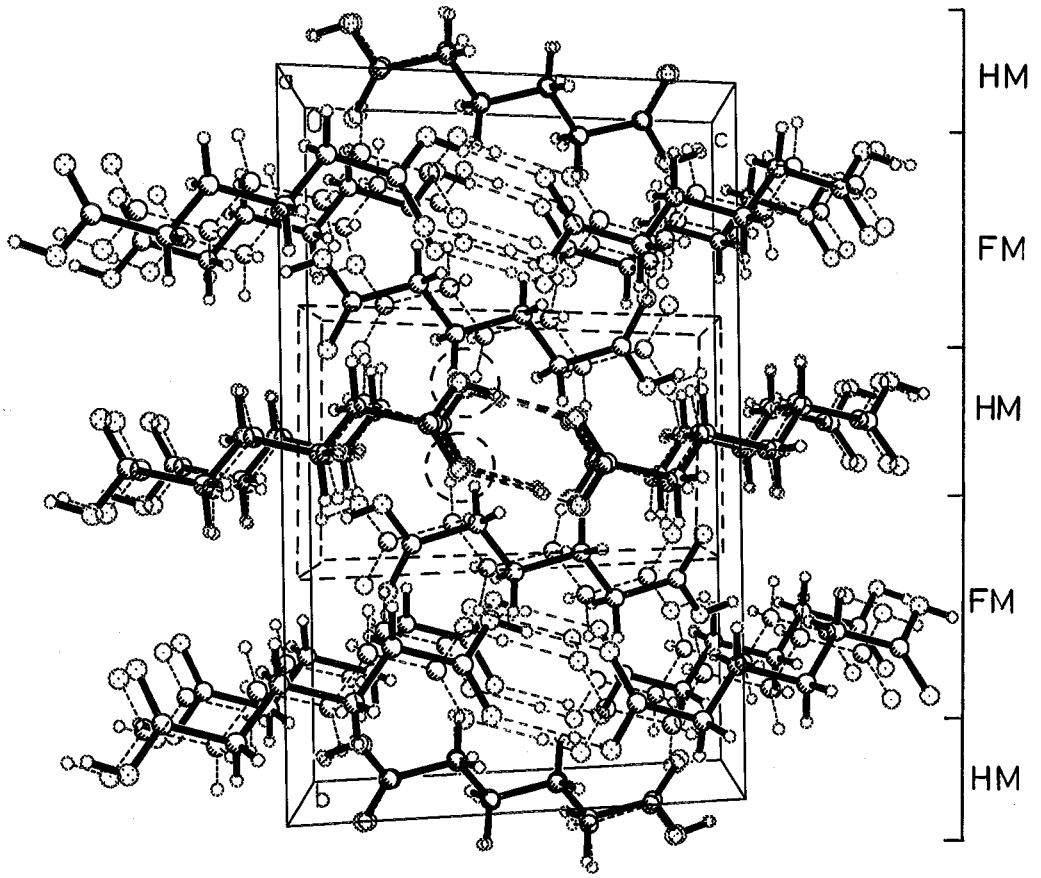

FIG. 3. Packing diagrams of the high- and low-temperature phases superimposed to visualise molecular displacements. High-temperature, dashed lines; low-temperature, solid lines. FM and HM denote domains generated by the full- and the half-molecule fragments of the low-temperature asymmetric unit. The unit cells are also shown.

ACKNOWLEDGMENTS

The authors acknowledge the support and encouragement given by Professor C. N. R. Rao, F.R.S. One of the authors (G.U.K.) is profoundly thankful to Professor Rao for suggesting to work in this interesting area of research.

REFERENCES

1. C. N. R. Rao and K. J. Rao, "Phase Transitions in Solids: An Approach to the Study of the Chemistry and Physics of Solids." McGraw-Hill, New York, 1978.
2. C. N. R. Rao, *J. Mol. Struct.* **292,** 229 (1993).
3. J. D. Dunitz, *Pure Appl. Chem.* **63,** 177 (1991).
4. Y. V. Mnyukh, *Mol. Cryst. Liq. Cryst.* **52,** 163 (1979).
5. P. J. L. Baudour, Y. Delugeard, and H. Caileau, *Acta. Crystallogr., Sect. B* **32,** 150 (1976).
6. A. T. H. Lenstra, C. Canalsenoy, K. Verhulst, and H. J. Geise, *Acta Crystallogr., Sect. B* **50,** 96 (1994).
7. P. Coppens and T. M. Sabine, *Mol. Cryst. Liquid Cryst.* **3,** 507 (1967).
8. C. N. R. Rao, S. Ganguly, and H. R. Swamy, *Croat. Chem. Acta* **55,** 207 (1982).
9. N. R. Jagannathan and C. N. R. Rao, *Chem. Phys. Lett.* **140,** 46 (1987).
10. J. D. Morrison and J. M. Robertson, *J. Chem. Soc.* 987 (1949).
11. J. Housty and J. Hospital, *Acta Crystallogr.* **18,** 693 (1965).
12. H. Ohki, N. Nakamura, and H. Chihara, *J. Phys. Soc. Jpn.* **57,** 382 (1988).
13. Siemens Analytical X-ray Instruments Inc., Madison, WI, 1995.
14. "SHELXTL (SGI version)," Siemens Analytical X-ray Instruments Inc., Madison, WI, 1995.